



# Water isotope ratio (d2H and d18O) measurements in atmospheric moisture using an optical feedback cavity enhanced absorption laser spectrometer

Rosario Iannone, D. Romanini, Olivier Cattani, Harro A.J. Meijer, E. R. T. Kerstel

## ► To cite this version:

Rosario Iannone, D. Romanini, Olivier Cattani, Harro A.J. Meijer, E. R. T. Kerstel. Water isotope ratio (d2H and d18O) measurements in atmospheric moisture using an optical feedback cavity enhanced absorption laser spectrometer. *Journal of Geophysical Research: Atmospheres*, 2010, 115, pp.D10111. 10.1029/2009JD012895 . hal-00563780

**HAL Id: hal-00563780**

**<https://hal.science/hal-00563780>**

Submitted on 7 Feb 2011

**HAL** is a multi-disciplinary open access archive for the deposit and dissemination of scientific research documents, whether they are published or not. The documents may come from teaching and research institutions in France or abroad, or from public or private research centers.

L'archive ouverte pluridisciplinaire **HAL**, est destinée au dépôt et à la diffusion de documents scientifiques de niveau recherche, publiés ou non, émanant des établissements d'enseignement et de recherche français ou étrangers, des laboratoires publics ou privés.

# 1 Water isotope ratio ( $\delta^2\text{H}$ and $\delta^{18}\text{O}$ ) measurements in atmospheric 2 moisture using an optical feedback cavity enhanced 3 absorption laser spectrometer

4 Rosario Q. Iannone,<sup>1</sup> Daniele Romanini,<sup>2</sup> Olivier Cattani,<sup>3</sup> Harro A. J. Meijer,<sup>1</sup>  
5 and Erik R. Th. Kerstel<sup>1</sup>

6 Received 26 July 2009; revised 30 October 2009; accepted 5 January 2010; published XX Month 2010.

7 [1] Water vapor isotopes represent an innovative and excellent tool for understanding  
8 complex mechanisms in the atmospheric water cycle over different time scales, and they  
9 can be used for a variety of applications in the fields of paleoclimatology, hydrology,  
10 oceanography, and ecology. We use an ultrasensitive near-infrared spectrometer,  
11 originally designed for use on airborne platforms in the upper troposphere and lower  
12 stratosphere, to measure the water deuterium and oxygen-18 isotope ratios *in situ*, in  
13 ground-level tropospheric moisture, with a high temporal resolution (from 300 s down to  
14 less than 1 s). We present some examples of continuous monitoring of near-surface  
15 atmospheric moisture, demonstrating that our infrared laser spectrometer could be used  
16 successfully to record high-concentration atmospheric water vapor mixing ratios in  
17 continuous time series, with a data coverage of ~90%, interrupted only for daily calibration  
18 to two isotope ratio mass spectrometry-calibrated local water standards. The  
19 atmospheric data show that the water vapor isotopic composition exhibits a high variability  
20 that can be related to weather conditions, especially to changes in relative humidity.  
21 Besides, the results suggest that observed spatial and temporal variations of the stable  
22 isotope content of atmospheric water vapor are strongly related to water vapor transport in  
23 the atmosphere.

24 **Citation:** Iannone, R. Q., D. Romanini, O. Cattani, H. A. J. Meijer, and E. R. Th. Kerstel (2010), Water isotope ratio ( $\delta^2\text{H}$   
25 and  $\delta^{18}\text{O}$ ) measurements in atmospheric moisture using an optical feedback cavity enhanced absorption laser spectrometer,  
26 *J. Geophys. Res.*, 115, XXXXXX, doi:10.1029/2009JD012895.

## 27 1. Introduction

28 [2] To obtain detailed knowledge of the hydrological  
29 cycle, information on all three phases of water is required.  
30 Isotopic analysis of atmospheric trace gases provides a  
31 valuable tool for resolving their budgets because the phys-  
32 ical, chemical, or biological processes involved fractionate  
33 isotopically in unique ways and leave characteristic isotopic  
34 signatures in the trace gas. In particular, water vapor iso-  
35 topes provide information concerning the mechanisms of  
36 processes that occur in the water cycle, such as evaporation  
37 at the surface of the Earth and subsequent transport and  
38 phase changes in the atmosphere.

39 [3] The Global Network for Isotopes in Precipitation  
40 (GNIP), founded in 1958 by the World Meteorological  
41 Organization and the International Atomic Energy Agency  
42 (IAEA), has been surveying the isotopic composition of

precipitation water since 1961 [Araguas Araguas *et al.*, 43  
1996]. The network consists of about 100 sampling sites 44  
around the world, including marine, coastal, and inland sta- 45  
tions. Through those measurements, some information has 46  
already been obtained about the isotopic composition of 47  
atmospheric moisture, assuming that application of the 48  
Rayleigh condensation model is valid: the isotope distribu- 49  
tion in precipitation is an “equilibrium proxy” for the one in 50  
the vapor phase. This assumption is based on the concept of 51  
temperature-dependent equilibrium isotope exchange effects. 52  
However, because precipitation predominantly occurs as 53  
discrete events in both space and time, sampling of liquid 54  
water does not provide an estimate of vapor isotopic com- 55  
position with high temporal resolution, and it does not pro- 56  
vide information on changes occurring between precipitation 57  
events, or in areas with low or even zero precipitation. This 58  
has motivated new efforts to obtain more data on the spatial 59  
and temporal variation in the isotopic composition of 60  
atmospheric moisture. 61

[4] A second network was thus initiated by the IAEA in 62  
1994. This network was named Moisture Isotopes in the 63  
Biosphere and Atmosphere and it is intended to complement 64  
and expand the GNIP ([http://www-naweb.iaea.org/naweb/ih/](http://www-naweb.iaea.org/naweb/ih/MIBA/IHS_MIBA_current.html) 65  
MIBA/IHS\_MIBA\_current.html). 66

<sup>1</sup>Centrum voor IsotopenOnderzoek, University of Groningen, Groningen, Netherlands.

<sup>2</sup>Laboratoire de Spectrométrie Physique, UMR 5588, Université J. Fourier Grenoble, CNRS, Saint Martin d'Hères, France.

<sup>3</sup>LSCE, IPSL CEA Saclay, Gif sur Yvette, France.

[5] Water-vapor isotope measurements can be used to reveal a possible relationship between water-vapor isotopes and ambient moisture. In addition, atmospheric humidity shows a diurnal pattern and it would be interesting to verify the existence of this variation in the isotopes signal. Ultimately, the information obtained in these atmospheric moisture isotope studies can be used to improve the representation of processes such as evaporation and condensation in climatic simulations.

[6] Isotopic variations in H<sub>2</sub>O vapor are usually reported as delta values, expressed in per mil (‰), giving the deviation of the ratio of the rare isotope to the most abundant isotope, relative to a standard. The internationally accepted standard material, used in hydrological applications, is known as Vienna standard mean ocean water (VSMOW) [Gonfiantini, 1978]. If we define  $R$  to be the ratio  $[^2\text{H}]/[^1\text{H}]$  or  $[^{18}\text{O}]/[^{16}\text{O}]$  in the sample or in the standard, we thus have

$$\delta = \left[ \frac{R_{\text{sample}} - R_{\text{standard}}}{R_{\text{standard}}} \right]. \quad (1)$$

Although the determination of the isotopic content of rainfall is a fairly straightforward process, measuring isotopic ratios in the vapor is not easily performed and requires sophisticated equipment.

[7] The conventional technique for this specific application generally involves the use of cold traps cooled to roughly  $-80^\circ\text{C}$  in order to collect water vapor, followed by laboratory isotope ratio mass spectrometry (IRMS) analyses. Jacob and Sonntag [1991] recorded almost continuous time series (sampling period of 1 or 2 days) of  $\delta^2\text{H}$  and  $\delta^{18}\text{O}$  in atmospheric water vapor at Heidelberg (Germany) over a time span of 8 years. We also cite the effort of He and Smith [1999], who sampled water vapor from a light aircraft above a forest in New England, Connecticut (United States), and Wang and Yakir [2000], who measured water-vapor stable isotopes to study evapotranspiration fluxes above canopies.

[8] Another option is to measure the water-vapor isotopic distributions from space using a satellite-based spectrometer. Worden et al. [2007] used the Tropospheric Emission Spectrometer on board the Aura spacecraft to obtain a characterization of the vertical profiles of  $^1\text{H}^{16}\text{O}^2\text{H}$  and  $\text{H}_2^{16}\text{O}$  in the tropical region. It is worth noting that both cryogenic whole air sampling and satellite remote sensing produce measurements with limited temporal resolution, spatial resolution, or both.

[9] Optical spectroscopy enables long time series of onsite measurements with high temporal coverage. Lee et al. [2005] carried out continuous measurements of  $\text{H}_2^{18}\text{O}/\text{H}_2^{16}\text{O}$  in atmospheric water vapor in New Haven, Connecticut (United States), using a commercial Campbell-Scientific tunable diode laser (TDL) gas analyzer. Later, Wen et al. [2008], extended this study to include measurements of  $\delta^2\text{H}$  using an upgraded version of the TDL analyzer. Griffith et al. [2006] used a Fourier transform infrared (FTIR) spectrometer to perform measurements of  $\delta^2\text{H}$  in an Australian eucalypt forest near Tumbarumba, New South Wales, in southeastern Australia. Both these works describe systems for measurement of atmospheric water vapor isotopes in real time, based on infrared spectroscopy. Both the Campbell Scientific and the FTIR instruments are fairly big and

require liquid nitrogen cooling for laser and/or detector operation.

[10] Finally, very recently, measurements of  $\delta^2\text{H}$  and  $\delta^{18}\text{O}$  of atmospheric moisture were carried out by Wang et al. [2009], whose aim was to calibrate an off-axis integrated cavity output spectrometer, manufactured by Los Gatos Research, Inc. (<http://www.lgrinc.com>). The precisions achieved with this instrument were  $\sim 0.1\text{‰}$  for  $^{18}\text{O}$  and  $0.4\text{‰}$  for  $^2\text{H}$ , for an averaging time of over 500 s. Continuous records of isotopic composition of water vapor were also reported by Galewsky et al. [2009], who performed in situ measurements at the Mauna Loa Laboratory in Hawaii. They used three laser spectrometers, of which two were commercial (Los Gatos Research, Inc., and Picarro, Inc., <http://www.picarro.com>), whereas the third laser-based spectrometer was developed at the Jet Propulsion Laboratory.

[11] Here we demonstrate that the infrared laser spectrometer we previously developed for airborne applications [Kerstel et al., 2006; Iannone et al., 2009b] can be successfully applied to the isotopic characterization ( $\delta^2\text{H}$  and  $\delta^{18}\text{O}$ ) of atmospheric, near-surface moisture through real-time and continuous measurements with an accuracy and precision comparable to that of cryogenic sampling and IRMS, but with a much higher temporal resolution. The instrument is lightweight (3 kg for the optical core, excluding the computer and pump) and small ( $\sim 25\text{ L}$ ), has a low power consumption ( $\sim 150\text{ W}$ ), and requires no liquid nitrogen, making it ideally suited for field operation. It has a large dynamic range of absorption measurement, a feature in common with the commercial Los Gatos Research and Picarro near-infrared water vapor isotope ratio spectrometers. In addition, all three spectrometers are able to operate autonomously, and the small size and the high degree of portability make the analyzers easily transportable to the field for use in in situ measurements.

[12] In the Los Gatos Research analyzer, the incoherent coupling to a very dense cavity mode structure produces a very low level of output signal compared to the other two techniques and, consequently, requires a fairly high laser power and a good signal detection system. Moreover, the optical cell necessarily incorporates very large diameter mirrors, which makes the gas cell volume large, and thus increases the pumping requirement, if the gas exchange time (which limits the instrument response time) must be kept short. Our spectrometer and the Picarro analyzer share the advantage of a very small cavity volume. An advantage of the particular technique used in our spectrometer is the inherent frequency calibration of the spectrum. For this purpose, the Picarro analyzer is equipped with a proprietary wavelength monitor module, which adds complexity and cost to the instrument. Calibration of the (relative) frequency scale is important in that it is a prerequisite for very precise model fits to the spectral absorption features, which generally improve the long-term reproducibility of the absorption measurements.

[13] We show preliminary measurements of water-vapor isotope ratios in ambient air, sampled at the rooftop of the Center for Isotope Research in Groningen, Netherlands ( $53^\circ 13'\text{N}$ ,  $6^\circ 33'\text{E}$ ) during two 1-week measurement campaigns, when the instrument was not needed within its designated project of airborne isotope ratio analysis of atmospheric moisture. Although the spectrometer performance was

below its optimum (the noise equivalent absorption, NEA, was almost a factor of 3 worse than what can be obtained with the same setup and some sample introduction issues were identified, as is discussed farther down), we use the data here to show the wealth of information that can be obtained with online continuous monitoring of atmospheric, and thus relatively high water content, moisture, which does not require the utmost sensitivity of the instrument. We demonstrate that the results substantially surpass a conventional offline cryogenic sampling strategy in terms of information content.

## 2. Methods

### 2.1. Experimental Setup

[14] In recent years, several laser spectroscopic methods have been proposed, developed, and optimized for isotopic investigations, especially in the infrared region [Kerstel, 2004; Kerstel and Gianfrani, 2008]. In this region, most molecular species exhibit strong vibrational-rotational absorption bands. This feature, combined with the use of diode lasers, enables the resolution of single spectral lines of a molecule and to discriminate between different isotopologues.

[15] The instrument used here was designed and constructed to use near-infrared diode laser absorption spectroscopy to detect water vapor isotopologues with a room temperature, distributed feedback laser (Laser Components GmbH) operating around  $1.39 \mu\text{m}$  ( $7184 \text{ cm}^{-1}$ ). The laser is tuned over a  $1 \text{ cm}^{-1}$  spectral range, enabling the nearly simultaneous registration of  $\text{H}_2\text{O}$  isotopologue spectral features, including rovibrational absorption lines belonging to  $\text{H}^{16}\text{OH}$ ,  $\text{H}^{17}\text{OH}$ ,  $\text{H}^{18}\text{OH}$ , and  $^{1}\text{HO}^2\text{H}$ . The  $\delta^{17}\text{O}$  measurements are not considered here since they do not, and in fact are not expected to, yield information beyond that provided by  $\delta^{18}\text{O}$  because of the relationship between  $^{17}\text{O}$  and  $^{18}\text{O}$  observed in all tropospheric meteoric waters [Meijer and Li, 1998]. In order to see deviations from this behavior in tropospheric, evaporated water, extremely high precision measurements of  $\delta^{17}\text{O}$  and  $\delta^{18}\text{O}$  are required, which are beyond the capabilities of this spectrometer [Barkan and Luz, 2007].

[16] The device uses the sensitive technique of optical feedback cavity enhanced absorption spectroscopy (OFCEAS) and was developed in collaboration with the University of Grenoble. Advantages of OFCEAS, compared to other laser spectroscopic techniques, include the large dynamic range, enabling isotope ratio measurements over almost three orders of magnitude in the water-vapor mixing ratio, and a small gas cell volume, enabling a fast gas exchange and spectrometer response. For a detailed description of the experimental apparatus we refer to a previous publication [Kerstel et al., 2006], whereas its principle of operation is described by Morville et al. [2005].

[17] The technique of CEAS yields a direct measurement of the wavelength-dependent absorption coefficient  $a$ , which can be written as the product of the number density  $n$ , the normalized line shape function  $f$ , the line strength  $S$ , and the absorption path length  $l$ :

$$a(\nu) = n(p, T) f(p, T, \nu - \nu_0) S(T) l, \quad (2)$$

where  $p$  and  $T$  represent the total pressure and temperature of the sample in the spectrometer cavity,  $\nu$  represents the laser frequency, and  $\nu_0$  represents the line-center frequency. Integration of the absorption coefficient over the entire line profile  $f$  (i.e., the “line area”) directly yields the number density of the associated species, assuming the line strength is known. The line strengths of the absorption lines used in this study, as well as their temperature and pressure dependencies, are all tabulated in the HITRAN database [Rothman et al., 2005]. The effective path length is determined by frequent calibration of the absorbance scale of the spectrometer by means of cavity ring down measurements [Kerstel et al., 2006].

[18] The mixing ratio is calculated assuming ideal gas behavior. The isotope ratios, instead, are given by the super-ratio of the absorption coefficients of the rare and abundant isotopologues in the sample and a reference material [Kerstel, 2004] and, thus, require no knowledge of the line strengths. For example, in the case of oxygen-18,

$$\delta^{18}\text{O} = \frac{[a(\text{H}^{18}\text{OH})/a(\text{H}^{16}\text{OH})]_{\text{sample}}}{[a(\text{H}^{18}\text{OH})/a(\text{H}^{16}\text{OH})]_{\text{reference}}} - 1. \quad (3)$$

We note that equation (3) differs from equation (1) in the use of molecular instead of atomic quantities. It can be shown that the molecular isotopologue abundance ratios,  $^2\text{R}_\text{M} = [\text{HO}^2\text{H}]/2[\text{H}_2\text{O}]$  for deuterium and  $^{17/18}\text{R}_\text{M} = [\text{H}_2^{17/18}\text{O}]/[\text{H}_2^{16}\text{O}]$  for oxygen-17/18, are in good approximation equal to their atomic counterparts (such as  $^2\text{R} = [^2\text{H}]/[^1\text{H}]$ ). This equivalence of molecular and atomic values is an even better approximation for the case of the “delta value” ( $\delta = R_{\text{sample}}/R_{\text{reference}} - 1$ ) of equation (3) [Kerstel, 2004].

[19] The reference ratio of the absorption coefficients is determined experimentally through periodic calibration measurements on local standard materials that are well characterized on the international, two-point VSMOW-SLAP (standard light Antarctic precipitation) isotope scale [Gonfiantini, 1984; Hut, 1987], as explained in more detail in section 2.2.

[20] The whole setup is housed in an insulated aluminum case, thermally regulated by two ribbon heaters (MINCO) to a temperature of  $32^\circ\text{C}$ . To facilitate thermal exchange, two ventilators are placed inside the box. A flow is established inside the gas cell by means of a molecular drag pump. The flow rate is adjusted via a manual valve, while the gas pressure inside the cell is stabilized independently of the flow by a forward pressure controller (Bronkhorst). The pressure is therefore kept stable at a value of 40 mbar. The small gas cell volume of  $\sim 20 \text{ mL}$  ensures a fast gas cell exchange ( $< 4 \text{ s}$ ) with a very modest pumping speed of  $150 \text{ mL/min}$  (Alcatel Drytel 1025) [Kerstel et al., 2006].

### 2.2. Calibration System

[21] Figure 1 represents a schematic of the gas handling system used to calibrate the measurement of the atmospheric water isotopes. The gas flow system basically has three operational modes: ambient air inlet and either one of two calibration gas streams. Outside ambient air was continuously drawn through the system by means of fused silica-coated (1/4-in. OD) tubing (O’Brien) leading from the rooftop of our laboratory (line 3). As the flow inside the



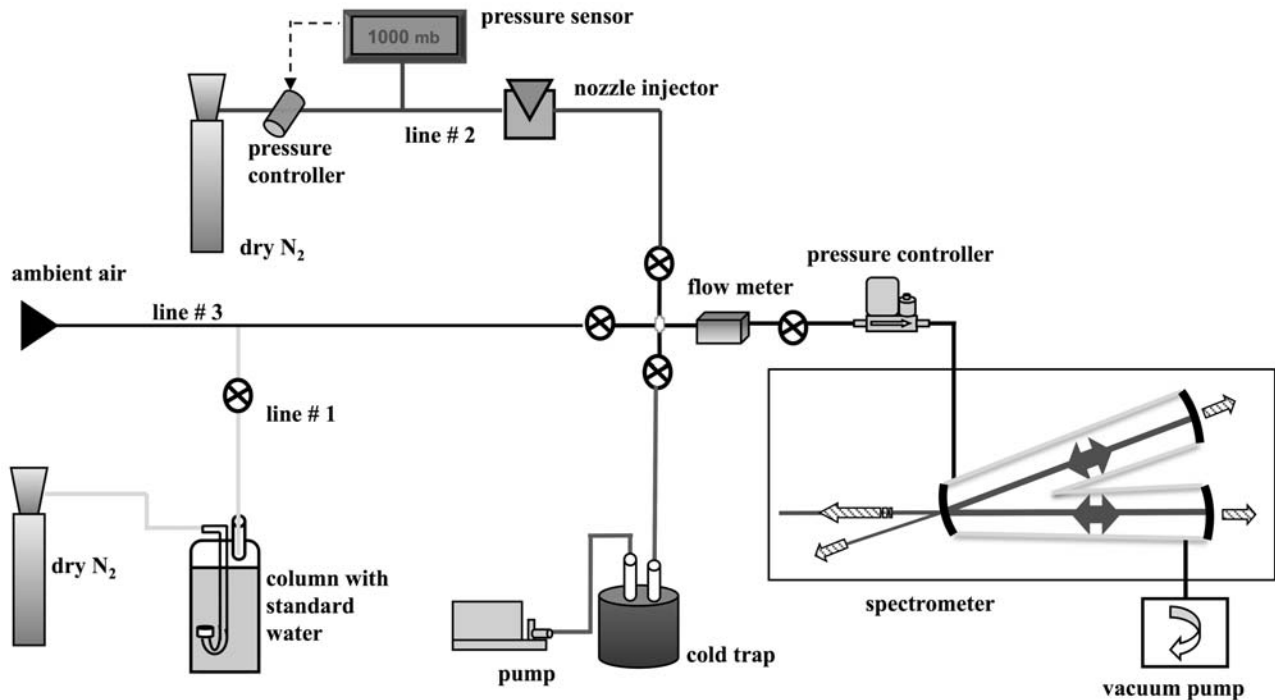


**Figure 1.** Sketch of the experimental arrangement used to calibrate the atmospheric measurements of water vapor isotope ratios. Three gas lines were used, one to lead atmospheric air to the laser spectrometer (line 3), and the other two for delivery of reference water vapor (lines 1 and 2), as explained in the text (section 2.2). The pressure controller establishes a pressure of 40 mbar inside the optical cell, whereas the flow was regulated to 150 mL/min by a metering valve at the exit of the spectrometer.

298 tube remains laminar, the length of the tube (10 m) does not  
 299 noticeably alter the overall system response time, which  
 300 was demonstrated to be 2 s in a series of measurements  
 301 carried out by switching between synthetic air and labora-  
 302 tory air. A 50  $\mu$ m nylon filter was inserted at the beginning  
 303 of the sampling line in order to eliminate particles from the  
 304 airstream.

305 [22] The atmospheric measurements were interrupted  
 306 once or twice daily for calibration measurements using two  
 307 local isotopic standard waters. The use of two reference  
 308 waters enables the calibration of the atmospheric moisture  
 309 measurements to a two-point isotope scale in a procedure  
 310 similar to the standard VSMOW-SLAP calibration proce-  
 311 dure described by Gonfiantini [1984] and Hut [1987].

312 [23] Two calibration lines were installed. In the case of  
 313 tropospheric water vapor characterized by a mixing ratio  
 314 higher than 5000 ppmv, as encountered during measure-  
 315 ments carried out in the month of July, calibration line 1 was  
 316 used to obtain a reference moist airstream with a mixing  
 317 ratio of 15,000 ppmv, comparable to that of the analyzed  
 318 atmospheric air. In this case, two different reference waters  
 319 of known isotopic composition, named GS-90 and GS-91,  
 320 were stored in two tall (~1 m) and narrow columns with a  
 321 volume of 2 L. The large volume of the bubblers guarantees  
 322 that the isotopic composition change, due to the departure of  
 323 water from the column in the form of vapor, is completely  
 324 negligible. The isotopic composition of the GS-90 and  
 325 GS-91 reference waters was determined by repeated

IRMS analyses in our Groningen laboratory. The isotope 326  
 ratios are  $\delta^2\text{H} = (-42.9 \pm 0.6)\text{‰}$  and  $\delta^{18}\text{O} = (-6.34 \pm 0.02)\text{‰}$  327  
 for GS-90, and  $\delta^2\text{H} = (-170.3 \pm 0.5)\text{‰}$  and  $\delta^{18}\text{O} = (-22.37 \pm$  328  
 $0.02)\text{‰}$  for GS-91. A flow of dry nitrogen (grade purity 329  
 5.0 UN 1066 nitrogen, water content  $<1$  ppmv), from a 330  
 high-pressure tank, was passed ("bubbled") through the 331  
 water after entering at the bottom of the column. The flow 332  
 rate through the water column was set at 150 mL/min. The 333  
 moist stream leaving the column, and subsequently diluted 334  
 with nitrogen from the same tank in order to arrive at total 335  
 water-vapor content similar to the analyzed air, was led 336  
 through the laser spectrometer. The dilution ratio was 337  
 determined by mass flowmeters, whereas the exact mixing 338  
 ratio in this case was determined by the temperature and the 339  
 gas pressure in the bubbler column. Using this scheme, the 340  
 isotope ratio of the moist air exiting the column is thus not 341  
 identical to the liquid water feed, but a fractionation factor 342  
 that depends on the water-vapor temperature must be taken 343  
 into account. The expected delta values for the GS-90 344  
 standard in the moist stream are  $-16.05\text{‰}$  and  $-121.3\text{‰}$  for 345  
 $\delta^{18}\text{O}$  and  $\delta^2\text{H}$ , respectively, given the fractionation factors of 346  
 $-9.71\text{‰}$  and  $-78.4\text{‰}$  for  $^{18}\text{O}$  and  $^2\text{H}$ , in that order, at a 347  
 temperature of 20°C [Majoube, 1971]. This is in good 348  
 agreement with the experimental values determined by 349  
 cryogenically collecting the GS-90 saturated water-vapor 350  
 sample at the top of the column and analyzing it by IRMS: 351  
 The reported isotope ratios in this case were  $(-16.37 \pm$  352  
 $0.02)\text{‰}$  for  $\delta^{18}\text{O}$  and  $(-120.7 \pm 0.4)\text{‰}$  for  $\delta^2\text{H}$ . The actual 353

isotopic composition during the calibration cycles was determined using fractionation factors corresponding to the measured temperature in the climatically controlled room.

[24] Gas line 2 was used for calibration of the spectrometer at a mixing ratio value of 4,500 ppmv during the January measurements when mixing ratios were typically <5000 ppmv. This independent calibration scheme also served as a check on the bubbler-generated, diluted calibration streams. It uses a nozzle injector (Microdrop GmbH) to inject water droplets of known size at a preset repetition frequency into a stream of dry nitrogen or synthetic air. A detailed description of this system is published elsewhere [Iannone *et al.*, 2009a]. The measurements were calibrated by the introduction of two local water standards, in this case GS-48 and GS-50. The GS-48 standard has an isotopic composition of  $(-43.3 \pm 0.3)\text{‰}$  for  $\delta^2\text{H}$  and  $(-6.52 \pm 0.03)\text{‰}$  for  $\delta^{18}\text{O}$ , while the GS-50 standard has a value of  $(-276.7 \pm 0.3)\text{‰}$  and  $(-35.01 \pm 0.03)\text{‰}$  for  $\delta^2\text{H}$  and for  $\delta^{18}\text{O}$ , respectively. Two nozzle injectors were employed in order to switch more rapidly between the two water standards.

[25] Finally, a comparison was made between our online laser spectrometer and the cryogenic sampling technique developed at the Commissariat à l'Énergie Atomique in Paris (CEA). The CEA device uses a trap cooled with an alcohol and dry ice slush and collects larger quantities of water, thus requiring a substantially larger flow ( $\sim 2$  L/min) than the laser spectrometer. Therefore, inlet line 3, which carries the ambient air, was equipped with a Y split. One part (150 mL/min) was led to the laser spectrometer, while the remainder went to the cryogenic collection device.

[26] Water-vapor samples were collected between 17 and 23 July 2007. Air continuously circulated through glass vapor traps immersed in an alcohol bath. The alcohol was kept at  $-80^\circ\text{C}$  by periodically adding liquid nitrogen or ice slush. Samples were collected during time intervals lasting between 10 and 13 h for a single sample.

[27] No more than a maximum of two samples per day could thus be collected (e.g., between 1300 and  $\sim 2200/2330$  h and between 2330 and  $\sim 1000$  h of the following day). The long sample time is due to the fact we wanted to collect 2–3 ml of water, a requirement for precise IRMS analyses at CEA. The calibration of the spectrometer using the bubblers was then performed in the time interval between 1000 and 1300 h and generally completed in less than 1.5 h.

[28] The water collected in the traps was quantitatively transferred to a small container by cryogenic vacuum distillation, within 12 h after collection. The collected water was successively analyzed for its isotope ratios on IRMS instrumentation at CEA. As an additional check, a small fraction of a number of samples was transferred to different vials and analyzed at the Centrum voor IsotopenOnderzoek (Groningen, Netherlands) with the IRMS capabilities of the biomedical laboratory (able to handle samples as small as 10  $\mu\text{L}$ ).

[29] Finally, during the intercomparison measurements, temperature and humidity sensors (Tinytag, TGP-4500) were mounted on the top of the building roof, close to our air intake, in order to have a continuous registration of these two atmospheric parameters. Furthermore, meteorological data were taken from the Royal Netherlands

Meteorological Institute (KNMI) Web site (accessible at <http://www.knmi.nl>).

### 3. Results and Discussion

Figure 2 shows an example of data of the ambient vapor isotope ratios for the period from 19 to 22 January 2007, in Groningen, Netherlands. Although the instrument has a time resolution of a few seconds (determined by the gas exchange rate), for these long time series we show one data point per 5 min. With an averaging time of 300 s, the measurement precision was determined to be 0.20‰ for  $\delta^{18}\text{O}$  and 0.75‰ for  $\delta^2\text{H}$  at a water mixing ratio of  $\sim 15,000$  ppm. These values are comparable to those reported previously for this spectrometer [Iannone *et al.*, 2009a, 2009b], despite the relatively high value of the NEA, which was determined to be approximately  $10^{-9} \text{ cm}^{-1} \text{ Hz}^{-0.5}$ , whereas a more typical value for this OFCEAS spectrometer is  $4 \times 10^{-10} \text{ cm}^{-1} \text{ Hz}^{-0.5}$  [Kerstel *et al.*, 2006].

For reasons of clarity, the calibration data are not shown in the graphs but the corresponding periods are clearly visible as gaps in the data record ( $\sim 10\%$  of the overall measurement time).

In Figure 2a, the black line (top curve) represents the relative humidity measured in our meteorological station of Lutjewad (about 40 km to the northwest of Groningen), while the shaded line (bottom curve) shows the ambient temperature. Figure 2b shows the amount of atmospheric water detected by our infrared laser spectrometer. It is worth noting how the spectrometer water-vapor mixing ratio follows a pattern consistent with the relative humidity, in agreement with the observation of small and often correlated variations in the outside temperature. Still, weather during this period was very variable and the relative humidity (RH) reached a maximum value of 93% between 19 and 20 January (day 1 and day 2), with an amount of rain of 2 mm. Between 20 and 21 January (day 2 and 3), rainfall reached 10 mm. The minimum value of 40% RH occurred by the end of 22 January (day 4), during a snow event.

Over this 4 day period of measurements,  $\delta^2\text{H}$  and  $\delta^{18}\text{O}$  values also exhibited a high degree of variability, attributed to the dynamic meteorological conditions. The isotope values of deuterium span a wide range from  $-90\text{‰}$  to  $-150\text{‰}$ , while the full range of variability of oxygen-18 measurements lies between about  $-16\text{‰}$  and  $-33\text{‰}$ . The  $\delta^{17}\text{O}$  measurements are not shown here since they are not expected to provide further information beyond that given by  $\delta^{18}\text{O}$  due to the very tight relation between  $\delta^{17}\text{O}$  and  $\delta^{18}\text{O}$  observed in all tropospheric water [see, e.g., Meijer and Li, 1998]. In fact, the  $^{17}\text{O}$  anomaly for our data, defined as  $\Delta^{17}\text{O} = \ln(1 + \delta^{17}\text{O}) - 0.528 \ln(1 + \delta^{18}\text{O})$ , assumes an average value of  $-0.4\text{‰}$ , equal to zero within the standard deviation of 1.6‰.

Continuous measurements of atmospheric water-vapor isotopes were also performed between 17 and 23 July 2007. At the time of recording the data, also 10 atmospheric water vapor samples were collected by a cryogenic sample method (see section 2.2). During the same period, time-integrated rainfall samples were collected and subsequently analyzed by mass spectrometry (see the discussion of Figure 4b here below). As before, the daily averaged weather conditions were taken from the KNMI Web site.

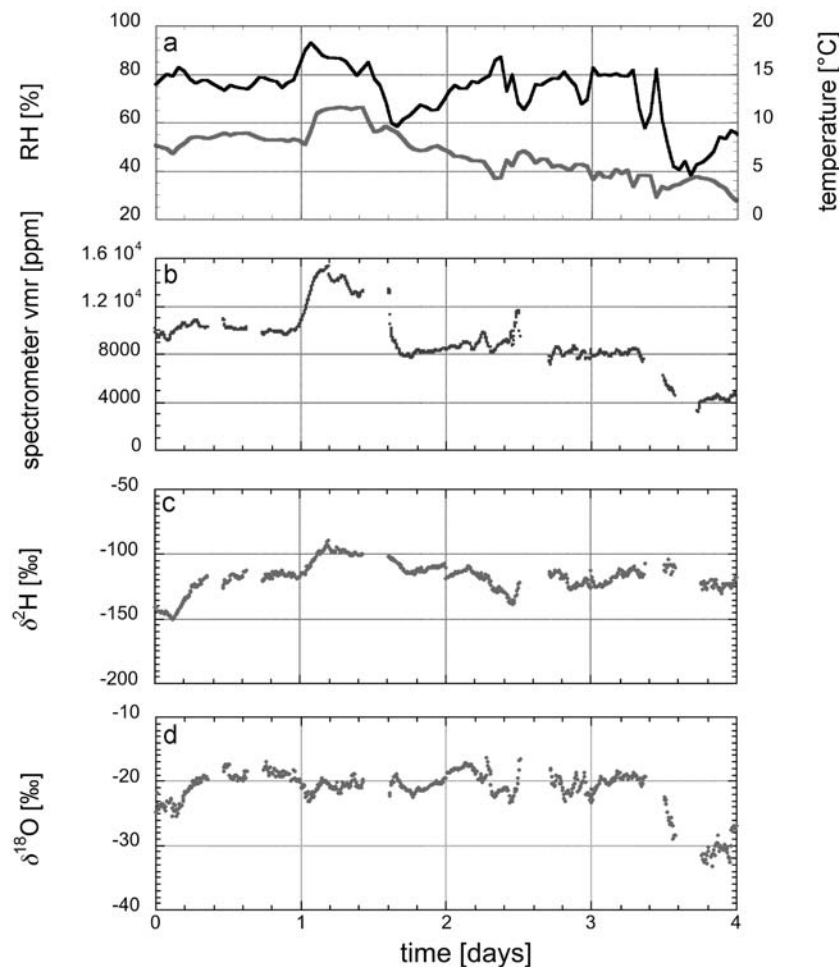


**Figure 2.** Continuous time series over 4 consecutive days with a 300 s time resolution: (a) ambient temperature and the simultaneously recorded relative humidity at the Lutjewad meteorological station (40 km NW of Groningen), (b) the volume mixing ratio of atmospheric air sampled from just outside the Groningen laboratory (53°N) as measured by the G2WIS spectrometer, (c)  $\delta^2\text{H}$ , and (d)  $\delta^{18}\text{O}$ . Two rain events and one snow event occurred during the 4 day measurement period (19–22 January). The horizontal arrows in Figure 2d indicate the precipitation events that occurred during these 4 days.

Figure 3a shows the 1-week time series of the relative humidity and ambient temperature, and the spectrometer water vapor content variation in the atmosphere,  $\delta^2\text{H}$ , and  $\delta^{18}\text{O}$  are shown in Figures 3b, 3c, and 3d, respectively. For clarity of presentation, the precipitation data are not shown. Over this week, there was considerable variability in the isotope ratios of  $\delta^2\text{H}$  and  $\delta^{18}\text{O}$ . The maximum values of  $\delta^2\text{H}$  and  $\delta^{18}\text{O}$  were about  $-79\text{‰}$  and  $-7.0\text{‰}$ , respectively, and the minimum values were  $-135\text{‰}$  and  $-23\text{‰}$ , respectively. [35] In Figure 3 the horizontal bars represent the  $\delta$  values determined by the cryogenic trap described in section 2.2. The extent of the bars corresponds to the sampling period. [36] To be able to compare the results of the cold trap and the laser spectrometer methods, mass-weighted average  $\delta^{18}\text{O}$  and  $\delta^2\text{H}$  values are obtained by weighing the delta values with the corresponding spectrometer water-vapor mixing ratios. The summation is over all delta values determined within the time frame of the cryogenic collection in question. The data are reported in Table 1. We notice that the overall deviation, given by the mean value of the

residuals, is  $-1.3\text{‰}$  ( $1.7\text{‰}$ ) for  $\delta^{18}\text{O}$  and  $+1.0\text{‰}$  ( $7.7\text{‰}$ ) for  $\delta^2\text{H}$ , where the values in parentheses give the standard deviation ( $n = 10$ ). No clear correlation is observed between the residuals of  $^{18}\text{O}$  and  $^2\text{H}$ . Similar differences between the isotope ratio measurements obtained by means of laser and those obtained by cryogenic collection and subsequent IRMS analysis have been reported previously by other authors. First, Lee *et al.* [2005] found an average difference of  $-1.77\text{‰}$  ( $1.75\text{‰}$ ) for their  $^{18}\text{O}$  measurements. This difference reduced to  $-0.36\text{‰}$  ( $1.43\text{‰}$ ) after correcting the data for incomplete cryogenic collection. Later, Wen *et al.* [2008] observed a disagreement between their TDL and cryogenic sampling techniques of up to  $-10.4\text{‰}$  and  $+4.9\text{‰}$  for deuterium and oxygen-18, respectively. Also, no correlation among the residuals of  $\delta^2\text{H}$  and  $\delta^{18}\text{O}$  could be seen [Wen *et al.*, 2008]. The authors attributed these differences to the difficulties of condensing out all sample water vapor passing through the cryogenic traps, as well as a combination of errors in both the laser spectrometer and IRMS analyses.

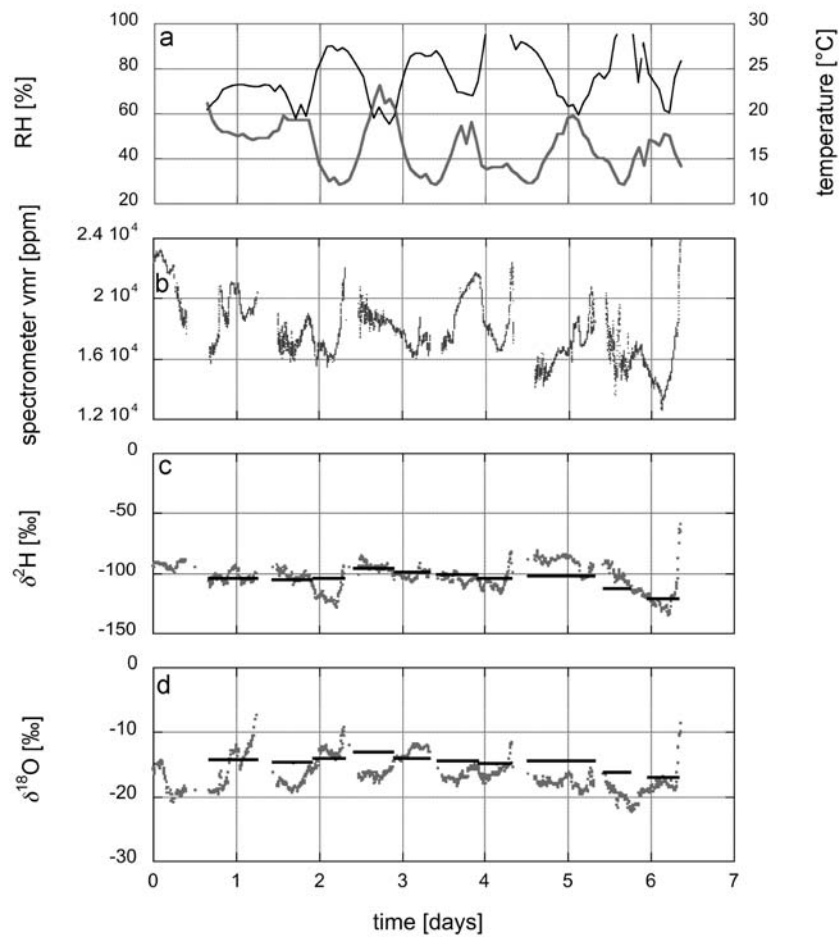


**Figure 3.** Time series of 300 s isotope composition of ambient water vapor measured with the laser spectrometer during the week of intercomparison with the cold-trap method (17–23 July 2007): (a) ambient temperature and the simultaneously recorded relative humidity just outside the Groningen laboratory (53°N, 6°E), (b) volume mixing ratio of atmospheric air as measured by the G2WIS spectrometer, (c)  $\delta^2\text{H}$ , and (d) the  $\delta^{18}\text{O}$ . The horizontal bars give the  $\delta^2\text{H}$  and  $\delta^{18}\text{O}$  values determined by the water-vapor cryogenic sampling system, with the horizontal extent of the bars indicating the sampling period.

[37] In our case, the discrepancy is most likely caused by condensation and the subsequent evaporation within the ambient air gas-inlet line. In particular, during the early morning hours the air temperature can drop below the dewpoint temperature, causing a phase change within the sampling stream and consequently altering the vapor isotope content. Although an attempt was made to heat the tubing line during the measurements, this failed to heat the total

**Table 1.** Comparison of the Water Vapor Mixing Ratio-Weighted  $\delta^2\text{H}$  and  $\delta^{18}\text{O}$  Values of the Atmospheric Water Vapor as Measured by G2WIS, and by Cryogenic Collection Followed by IRMS Analysis, for the Data Shown in Figure 3 (Collected from 17 to 23 July 2007)<sup>a</sup>

Samples	$\delta^2\text{H}_{\text{IRMS}}$ (‰)	$\delta^2\text{H}_{\text{LS}}$ (‰)	$\Delta^2\text{H}_{\text{LS-IRMS}}$ (‰)	$\delta^{18}\text{O}_{\text{IRMS}}$ (‰)	$\delta^{18}\text{O}_{\text{LS}}$ (‰)	$\Delta^{18}\text{O}_{\text{LS-IRMS}}$ (‰)	$v_{\text{H}_2\text{O}}$ (ppm)
1	−104.2	−102.9 (4.6)	−1.3	−14.3	−14.9 (3.3)	0.6	19098
2	−105.7	−104.5 (4.5)	−1.2	−14.8	−17.2 (1.2)	2.4	17449
3	−104.5	−117.9 (7.5)	13.4	−14.2	−13.0 (1.5)	−1.2	17300
4	−95.8	−96.1 (3.8)	0.3	−13	−16.1 (1.0)	3.1	18164
5	−99.9	−102.1 (3.3)	2.7	−14.1	−12.7 (0.9)	−1.4	17108
6	−101.3	−104.9 (3.4)	3.6	−14.5	−16.6 (0.9)	2.1	19786
7	−104.8	−107.6 (8.0)	2.8	−15	−16.1 (1.3)	1.1	18543
8	−102.6	−91.4 (6.1)	−11.2	−14.5	−17.9 (0.8)	3.4	16671
9	−112.9	−99.3 (6.0)	−13.6	−16.2	−19.2 (1.0)	3.0	16907
10	−121.9	−116.3 (13.7)	−5.6	−17	−17.3 (2.3)	0.3	15962
Mean			1.00			−1.3	
Standard deviation			7.8			1.7	
Standard error			2.4			0.55	

<sup>a</sup>The standard deviations are given in parentheses. IRMS, isotope ratio mass spectrometry; LS, laser spectrometer.



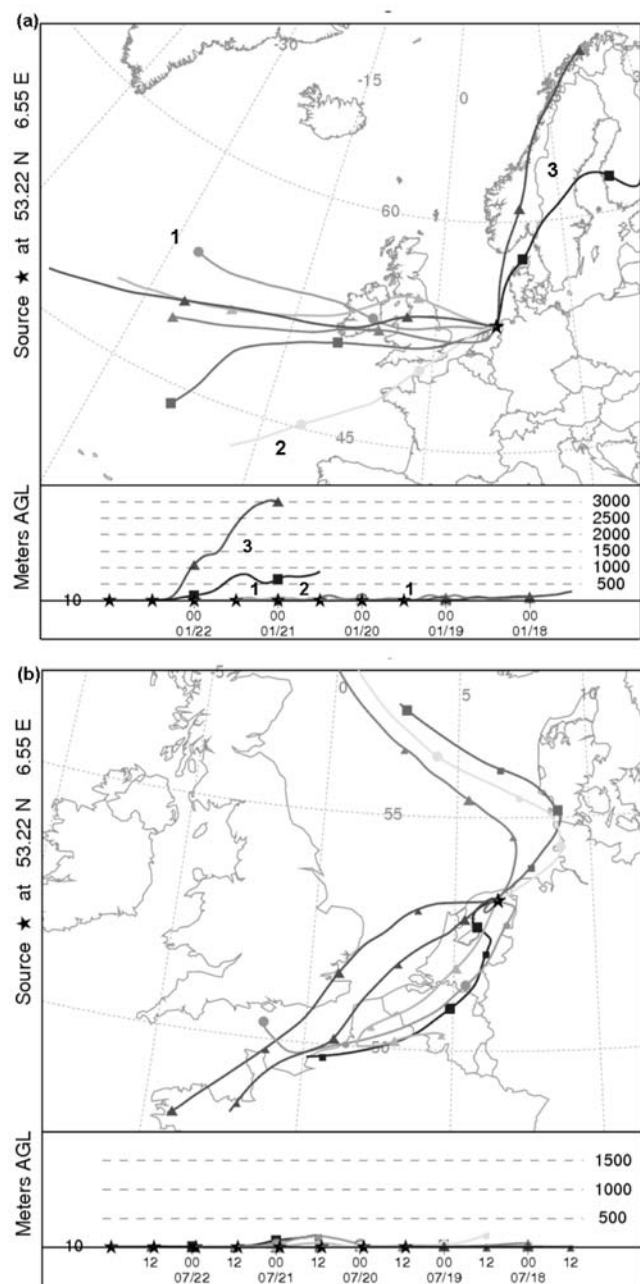


**Figure 4.** Twenty-four-hour-long backward trajectories produced by the NOAA HYSPLIT model. Two trajectories were calculated per day, one ending at 1200 and the other at 2400, for the two measurement periods: (a) 19–22 January and (b) 17–23 July 2007. Individual trajectories can be identified by their end time as is done in the bottom of each of Figures 4a and 4b. Trajectories start at 10 m above the ground. The boundary layer extended from 10 to 3000 m and from 10 to 1500 m for the months of January and July, respectively.

length of the inlet tube to temperatures above the high summertime temperatures registered on some of the days. The condensation of water vapor inside the inlet line is particularly apparent in Figure 3 during the early morning hours of days 2, 3, 5, and 7 by a rapid increase in the

measured mixing ratio beyond that predicted by the relative humidity and temperature records, and sharply increasing isotope ratio signals (especially visible in the  $^{18}\text{O}$  record). We believe that these excursions are due to the fact that the liquid water, which formed earlier in the gas line during periods of high outside temperatures, starts to evaporate faster when the atmospheric water content decreases during periods that combine a low outside temperature with a low RH. Since, in all cases, these periods of excessively high observed values of the volume mixing ratio are followed immediately by a calibration cycle of the spectrometer, the instrument is, as it were, reset. The flushing of the spectrometer with dry air, as part of the calibration cycle, effectively removes the excess humidity in the inlet line. The remainder of the data set is therefore believed to be still largely representative of outside atmospheric moisture.

[38] When comparing the data between January and July, a first difference to highlight concerns the variations in the RH. During most of the days in the winter period the water vapor content is fairly constant, whereas consistently higher water-vapor mixing ratios are observed during daytime than during nighttime in the summer season. This clear diurnal variation is not observed in the January data, in agreement with a strong diurnal temperature signal during the summertime measurements, which is absent in the winter data set.

[39] It is noteworthy, however, that also during the winter experiment, the RH reached high values (on one occasion as high as 93%), and the absence of a diurnal cycle in this case can be explained by large-scale transport and mixing of air masses rather than the local meteorological conditions. This interpretation of the data finds its origin in Figures 4a and 4b, which show backward trajectories computed using the NOAA Hybrid Single Particle Lagrangian Integrated Trajectory (HYSPLIT) model (available at <http://www.arl.noaa.gov/HYSPLIT.php>) [Draxler, 1992; Draxler and Hess, 1998]. The figures show that, during winter, air originates from both the western and southern Atlantic Ocean (area 1 and 2, respectively), as well as on some occasions from land regions in Norway (area 3). During summer, although the origin of air masses is variable, the direction of the majority of the back trajectories is toward the south.

[40] The variations of the deuterium and oxygen-18 isotope ratios in the atmospheric moisture are shown in Figures 5a and 5b, which show  $\delta^2\text{H}$  versus  $\delta^{18}\text{O}$  for the January and July measurements, respectively. In Figure 5, the global meteoric waterline (GMWL) is shown together with an evaporated waterline, with a slope of 4.5, intended here as a point of reference for the measured isotope ratios.

[41] The GMWL describes the globally averaged stable isotope composition of precipitation. During the evaporation of meteoric water, relative humidity is the major factor determining the isotopic composition of the atmospheric vapor besides temperature and wind speed. Humidity affects oxygen and hydrogen differently, such that the slope of the evaporation line varies due to changes in water-vapor mixing ratio content. This occurs because evaporation is partly a nonequilibrium process and, particularly, because lower relative humidity leads to a faster rate of evaporation and, consequently, the kinetic fractionation will be greater.

[42] From Figure 5a, it is clear that the individual  $\delta$  values of  $^2\text{H}$  and  $^{18}\text{O}$  are located slightly above the GMWL. The

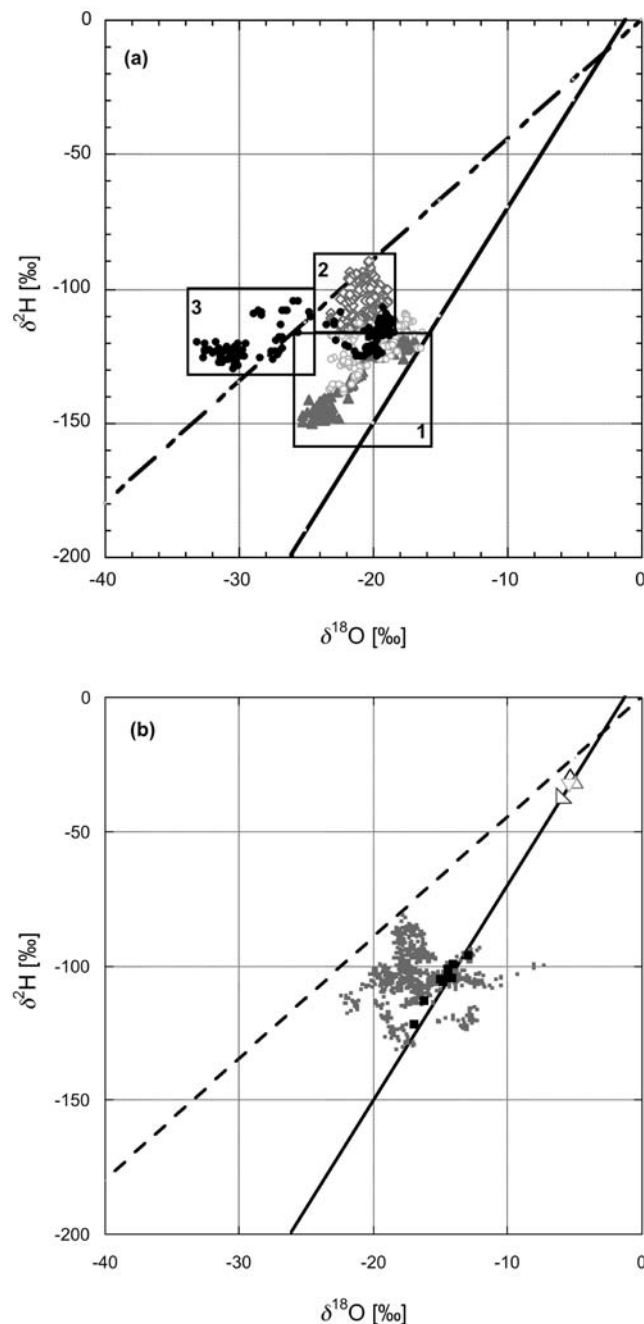


**Figure 5.** The meteoric relationship for  $^{18}\text{O}$  and  $^2\text{H}$  in water vapor (a) between 19 and 22 January 2007 (19 January 2007, solid triangles; 20 January 2007, open diamonds; 21 January 2007, open circles; 22 January 2007, solid circles) and (b) between 17 and 23 July 2007. In Figure 5a the three rectangular shapes indicate three different groups of data, each corresponding to a different humidity ranges (40%–60%, area 3; 60%–80%, area 2; and finally 80%–100%, area 1). Data suspected of condensation in the gas line are excluded from Figure 5b. Furthermore, in Figure 5b, the open triangles represent the isotopic composition of the rain events of this week, whereas the solid squares give the isotopic composition of the atmospheric samples collected by the cryogenic sampling system. For comparison, the GMWL (continuous line) and the evaporated water line (dashed line) are shown.

isotope measurements are identified by day: 19 January 590  
2007 (solid triangles), 20 January 2007 (open diamonds), 591  
21 January 2007 (open circles), and 22 January 2007 (solid 592  
circles). Three different groups of data can be identified, each 593  
corresponding to a different source area, which becomes 594  
apparent when the data are correlated with the back trajec- 595  
tories of Figure 4a. In fact, on 19 and 21 January, the air 596  
masses are originating from the western Atlantic Ocean 597  
(area 1); on 20 January, the back trajectory has its origin 598  
over the southern Atlantic Ocean (area 2); whereas on 22 599  
January, the air comes from Scandinavia (area 3). The dif- 600  
ferent source regions of the air masses are also reflected in 601  
the local RH level, which is clearly not determined by the 602  
local temperature only (cf. Figure 2, top). In fact, the three 603  
different areas correspond to three RH ranges: from 40% to 604  
60% (area 3), from 60% to 80% (area 2), and finally from 605  
80% to 100% (area 1). The plot of  $\delta^{18}\text{O}$  versus  $\delta^2\text{H}$  yielded 606  
a significant ( $r = 0.92$ ) straight-line relationship for the data of 607  
area 1. As well, the linear regression equation for the data of 608  
the second area shows a positive correlation ( $r = 0.68$ ) 609  
between the  $\delta^{18}\text{O}$  and  $\delta^2\text{H}$  of the water vapor. Finally, a 610  
similar but slightly lower correlation ( $r = 0.56$ ) is observed 611  
between deuterium and oxygen-18 in the data belonging to 612  
the third area. 613

[43] Figure 5b shows, besides the measured atmospheric 614  
moisture  $\delta^{18}\text{O}$  and  $\delta^2\text{H}$  isotope ratios, the four collected rain 615  
samples (triangles). The solid squares represent instead the 616  
isotopic composition of the atmospheric water vapor mea- 617  
sured by cryogenic collection and subsequent IRMS anal- 618  
ysis. Both the laser spectrometer and the IRMS data lie 619  
significantly closer to the GMWL compared to the data of 620  
January. In particular, as for the laser spectrometer data, the 621  
IRMS data are also found above the GMWL. The best fit 622  
through the IRMS data defines a slope  $\delta^2\text{H}/\delta^{18}\text{O}$  equal to 623  
6.3 ( $\pm 0.6$ ). This is a consequence of the higher RH. During 624  
this summer week, the humidity level reached values of 625  
about 96% in a strong diurnal cycle, and rain events 626  
occurred during the night from 17 to 18 July, and on 20, 21, 627  
and 22 July. These precipitation events are the main cause of 628  
variation of  $\delta^{18}\text{O}$  and  $\delta^2\text{H}$ . Precipitation leads to a more 629  
negative isotopic composition of the remaining vapor, while 630  
the increased humidity reduces the evaporation of local 631  
surface water. Moreover, rain events are generally linked to 632  
the arrival of different (warmer) air masses. 633

[44] It should be noted that the laser spectrometer isotope 634  
data show significantly higher variation than the cryogeni- 635  
cally collected samples. This is mostly due to the fact that 636  
the cryogenic collection method suffers from a strong bias 637  
toward high water content periods, especially given the 638  
extremely long sample collection times that were required to 639  
collect an amount of liquid water sufficiently large for iso- 640  
topic analysis at the CEA laboratory in Paris. 641

[45] Figures 5a and 5b are thus in good agreement with 642  
theoretical considerations according to which high levels of 643  
humidity result in a better isotope equilibrium between 644  
liquid and vapor and a MWL with a slope closer to 8 [Clark 645  
and Fritz, 1997]. 646

[46] In addition, it is possible to observe the influence of 647  
air originating from land regions in Scandinavia on the 648  
isotopic signature during the week in January. In particular, 649  
the arrival of these relatively dry air masses from north- 650  
westerly regions results in strong changes in the  $\delta^{18}\text{O}$  of 651

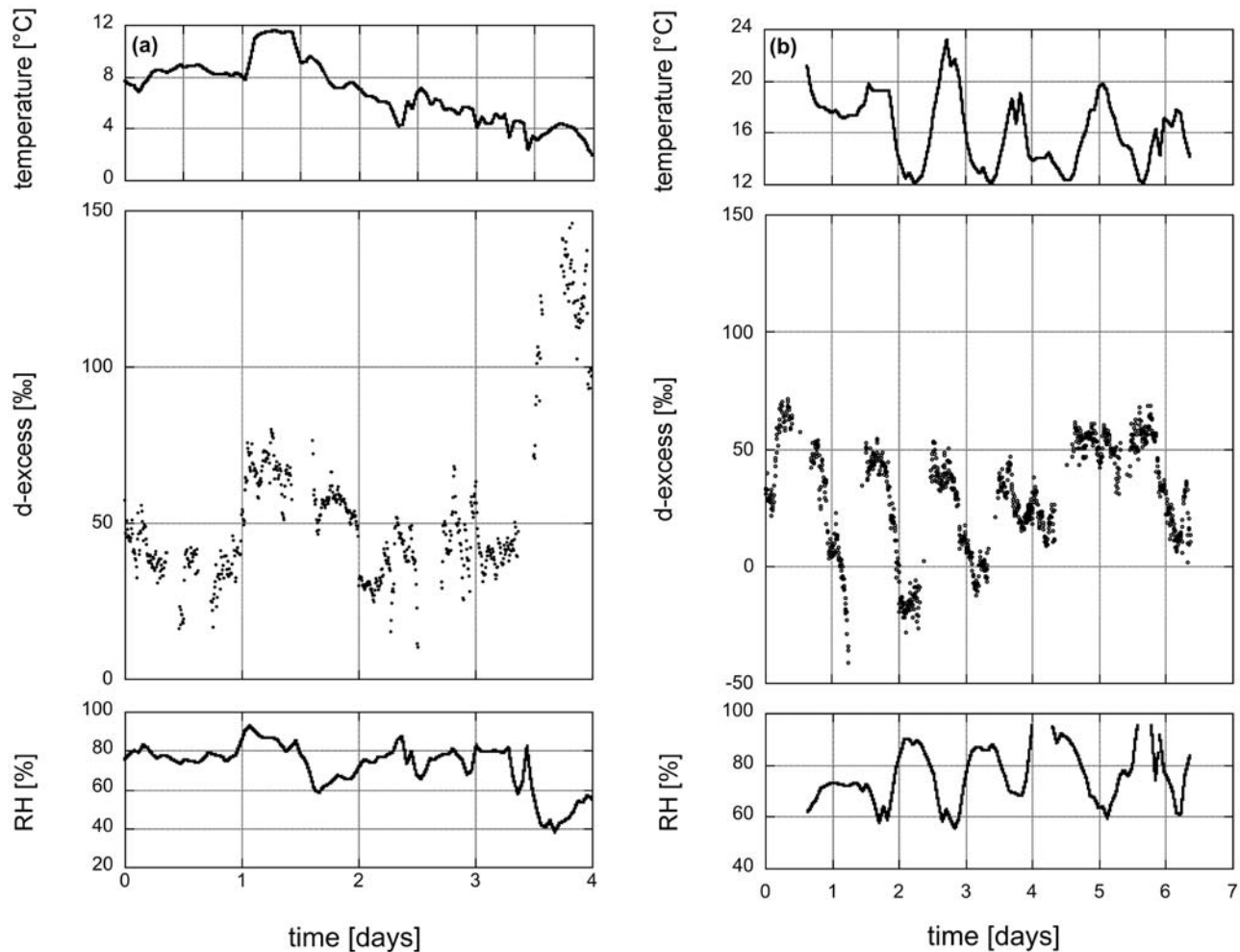


**Figure 6.** Time series of  $d$  excess based on the laser spectrometry method for (a) 19–22 January and (b) 17–23 July 2007: (top) ambient temperature and (bottom) relative humidity.

atmospheric water vapor. In fact, data of the second half of the day on 22 January (Figure 5a) have  $\delta^{18}\text{O}$  values that are consistently far from the GMWL. As a matter of fact, this necessarily indicates that (isotope) fractionation in the hydrologic cycle during this part of the day is not governed by liquid-vapor equilibrium. Jouzel and Merlivat [1984] proposed that nonequilibrium condensation becomes significant when sublimation on ice crystals occurs. These data, in fact, come from a period of a cold front passage during which snowfall occurred, corresponding to a sharp decreasing of the humidity as shown in Figures 2 (top) and 4a. This snow event explains why  $\delta^{18}\text{O}$  is so much lower compared to the previous period.

[47] During these particular meteorological conditions, the decrease in the  $\delta^2\text{H}$  value is less remarkable than that for  $^{18}\text{O}$ . This can be explained in terms of higher deuterium excess, defined as  $d = \delta^2\text{H} - 8 \cdot \delta^{18}\text{O}$  [Dansgaard, 1964], due to a strong kinetic evaporation, which takes place into unsaturated air. Vapor generated under low-humidity conditions has a high deuterium excess, as a result of the fact that the relative contribution of kinetic fractionation is larger for  $^{18}\text{O}$  than for  $^2\text{H}$  [Araguás Araguás et al., 2000]. This is very visible in Figure 6a, where the deuterium excess, for the January week, is graphed with the ambient temperature

and the RH. Typical values of  $d$  excess in rain samples in the Groningen region vary between 10‰ and 30‰. In our case, since the data define a  $\delta^2\text{H}/\delta^{18}\text{O}$  slope  $< 8$ , the  $d$  excess shows higher values. During the week in January, the deuterium excess ranged between +20‰ and +75‰ for most of the measurements period, except for the second half of the last day (22 January), where  $d$  excess reached values up to +125‰, indicating extreme low-moisture conditions. High values of  $d$  excess were also found by Angert et al. [2008]. In their publication they discuss results of measurements of the isotopic composition of atmospheric water vapor performed over 9 years (1998–2006). Although the temporal resolution is not very high, they report  $d$  excess values up to +50‰ during wintertime. The measurements were carried out in Israel, at which latitude one would normally expect to see lower deuterium excess values than at the higher latitude of our study. More important, the cryogenic collection method of the Israeli study is strongly biased toward high humidity (since during periods of high humidity more water is collected than during equally long low-humidity periods) and, thus, low deuterium excess, exacerbated by the long data collection times. From Figure 6a, we thus conclude that the  $d$  excess increases as the RH under which the evaporation occurred decreases. A plot of the  $d$  excess versus the



local RH shows a statistically significant correlation ( $r = 0.60$ ) under dry winter conditions. In addition, air masses with different moisture characteristics, due to their different origins, have higher  $d$  excess values and the  $d$  excess value can provide specific information to identify the mixing of evaporated air in the atmosphere.

[48] Figure 6b shows  $d$  excess for the week in July compared with temperature and humidity. During these summertime measurements, the  $d$  excess was negatively correlated with the RH with a correlation coefficient of 0.48. If the humidity is low,  $d$  excess values are high. In contrast,  $d$  excess values corresponding to high humidity are low. Again we see that the  $d$  excess may give insight into the RH deficit in air masses.

[49] These observations are in good agreement with the work of Uemura *et al.* [2008], who determined deuterium excess of atmospheric water vapor above the Southern Ocean in order to provide detailed knowledge of ocean surface conditions.

#### 4. Conclusion

[50] We have applied our instrument, originally designed for the in situ isotope analysis of stratospheric water vapor, to continuous, ground-based atmospheric water-vapor isotope measurements.

[51] Two approximately 1 week long data sets were recorded, one in January and the other in July 2007. The July data set was compared to IRMS analyses on moisture samples collected simultaneously by a cryogenic technique. Differences between the two different measurement strategies are attributed to condensation in the inlet line that affects mostly the laser measurements, as well as to incomplete sample collection in case of the cryogenic method. Thanks to the high time resolution of the laser method, as well as its continuous measurement nature, the inline condensation events are easily identified in both the volume mixing ratio and the isotope ratio records. The data sets also make it very apparent that the cryogenic technique is strongly biased toward high-water-concentration data and thus misses many of the most interesting features at low-water-volume mixing ratios visible in the continuous, high-resolution record.

[52] A strong positive relationship is observed between the isotopic composition of the water vapor and its mixing ratio, suggesting that the RH is the main meteorological parameter controlling the isotope distribution near the surface, as has been demonstrated previously in other related studies [Angert *et al.*, 2008; Jacob and Sonntag, 1991; White and Gedzelman, 1984].

[53] Even with the relatively small data set of this study, interesting differences between the behavior of the isotope signals in the winter and summer seasons are apparent. In particular, we observe that in summer the evaporation and the precipitation processes affect both deuterium and oxygen-18 simultaneously. High temperatures and high levels of humidity result in a near-isotopic equilibrium between air moisture and precipitation. Furthermore, the summer data show a clear diurnal cycle, in contrast to the winter data. In the wintertime, on the contrary, the interaction of fresh dry air from northwest of Groningen with western Atlantic Ocean air masses makes the change in the deuterium and oxygen-18 isotopes decoupled to a larger extent than is the

case in the summer season. For this reason also, the atmospheric moisture shows a large deuterium excess in winter.

[54] Nowadays, measurements of water vapor isotopes have become a significant topic in several fields of research, for example, in hydrology and ecology. With the introduction of laser technology, it has become increasingly possible to perform simultaneous in situ measurements of  $\delta^2\text{H}$  and  $\delta^{18}\text{O}$  in water vapor, making the optical isotope ratio technique definitely competitive with IRMS. Water-vapor isotope samples obtained with a cryogenic system, and subsequently analyzed with IRMS, can provide only an episodic picture of the weather conditions, which may turn out to be insufficient for reliable conclusions concerning changes in atmospheric water vapor.

[55] So far, the calibration of a laser spectrometer to measure water-vapor isotopes in near-surface atmospheric air has been most commonly done by means of a dew point generator [Lee *et al.*, 2005; Wen *et al.*, 2008]. This requires the knowledge of temperature-dependent isotope fractionation factors since the isotopic composition of the vapor is related to that of the liquid in the reservoir, and the need of relatively large quantities of water involved makes this procedure relatively expensive and quite unsuitable for field applications. The microdrop method developed by us can be easily extended to higher volume mixing ratios and is likely to become an important alternative to the dew point generator [Iannone *et al.*, 2009a]. The problems encountered with condensation in the inlet tubing during the summertime measurements in this preliminary study are easily resolved by properly heating the entire length of the inlet tube (e.g., by Ohmic heating) or by reducing the pressure in the inlet tube immediately after the air intake.

[56] Monitoring the stable isotope composition of atmospheric water vapor can provide a continuous record of valuable data on the atmospheric hydrological cycle. This will help to further understand the functioning of, and interactions between, the water cycle and other biogeochemical cycles, which in combination with retrieved observations by satellites will enable global mapping of the water cycle.

[57] **Acknowledgments.** The present work was funded by the Dutch Foundation for Fundamental Research on Matter (FOM, program number 99MAP10). We are grateful to Henk Been and Bert Kers for their excellent technical support. We also greatly appreciate the most helpful comments on the manuscript made by the anonymous reviewers.

#### References

- Angert, A., J.-E. Lee, and D. Yakir (2008), Seasonal variations in the isotopic composition of near-surface water vapour in the eastern Mediterranean, *Tellus*, doi:10.1111/j.1600-0889.2008.00357.
- Araguas Araguas, L., P. Danesi, K. Froehlich, and K. Rozanski (1996), Global monitoring of the isotopic composition of precipitation, *J. Radioanal. Nucl. Chem.*, 205, 189–200, doi:10.1007/BF02039404.
- Araguás-Araguás, L., K. Froehlich, and K. Rozanski (2000), Deuterium and oxygen-18 isotope composition of precipitation and atmospheric moisture, *Hydrol. Process.*, 14, 1341–1355, doi:10.1002/1099-1085(20000615)14:8<1341::AID-HYP983>3.0.CO;2-Z.
- Barkan, E., and B. Luz (2007), Diffusivity fractionations of  $(\text{H}_2\text{O})\text{-O-16}/(\text{H}_2\text{O})\text{-O-17}$  and  $(\text{H}_2\text{O})\text{-O-16}/(\text{H}_2\text{O})\text{-O-18}$  in air and their implications for isotope hydrology, *Rapid Commun. Mass Spectrom.*, 21(18), 2999–3005, doi:10.1002/rcm.3180.
- Clark, I. D., and P. Fritz (1997), *Environmental Isotopes in Hydrogeology*, CRC Press, Boca Raton, FL.
- Dansgaard, W. (1964), Stable isotopes in precipitation, *Tellus*, 16, 436–438, doi:10.1111/j.2153-3490.1964.tb00181.x.



- Draxler, R. R. (1992), *Hybrid Single-Particle Lagrangian Integrated Trajectories (HY-SPLIT): Version 3.0—User's Guide and Model Description*, Tech. Memo. ERL ARL-195, p. 26 and Appendices. Environ. Res. Lab. (NOAA), Boulder, Colo.
- Draxler, R. R., and G. D. Hess (1998), An overview of the HYSPLIT 4 modelling system for trajectories, dispersion and deposition, *Aust. Meteorol. Mag.*, 47, 295–308.
- Galewsky, J., D. Noone, Z. Sharp, and J. Woerden (2009), Water vapor isotopes measurements at Mauna Loa, Hawaii: Comparison of laser spectroscopy and remote sensing with traditional methods, and the need for ongoing monitoring, paper presented at European Geosciences Union General Assembly 2009, Vienna, 19–24 April.
- Gonfiantini, R. (1978), Standards for stable isotope measurements in natural compounds, *Nature*, 271, 534–536, doi:10.1038/271534a0.
- Gonfiantini, R. (1984), Report of the advisory group meeting on stable isotope reference samples for geochemical and hydrological investigations, Int. At. Energy Agency, Vienna.
- Griffith, D. W. T., I. Jamie, M. Esler, S. R. Wilson, S. D. Parkes, C. Waring, and G. W. Bryant (2006), Real-time field measurements of stable isotopes in water and CO<sub>2</sub> by Fourier transform infrared spectrometry, *Isotopes Environ. Health Stud.*, 42, 9–20, doi:10.1080/10256010500503098.
- He, H., and R. B. Smith (1999), Deuterium in water vapor evaporated from a coastal salt marsh, *J. Geophys. Res.*, 104(D9), 11,675–11,673, doi:10.1029/1998JD100108.
- Hut, G. (1987), Report to the director general, Int. At. Energy Agency, Vienna.
- Iannone, R. Q., D. Romanini, S. Kass, H. A. J. Meijer, and E. R. Th. Kerstel (2009a), A microdrop generator for the calibration of a water vapor isotope ratio spectrometer, *J. Atmos. Oceanic Technol.*, 26, 1275–1288, doi:10.1175/2008JTECHA1218.1.
- Iannone, R. Q., S. Kass, M. Chenevier, H.-J. Jost, D. Romanini, H. A. J. Meijer, and E. R. T. Kerstel (2009b), Development and airborne operation of a compact water isotope ratio infrared spectrometer, *Isotopes Environ. Health Stud.*, 45, 303–320, doi:10.1080/10256010903172715.
- Jacob, H., and C. Sonntag (1991), An 8-year record of the seasonal variation of <sup>2</sup>H and <sup>18</sup>O in atmospheric water vapor and precipitation at Heidelberg, Germany, *Tellus*, 43B, 291–300.
- Jouzel, J., and L. Merlivat (1984), Deuterium and oxygen 18 in precipitation: Modeling of the isotopic effects during snow formation, *J. Geophys. Res.*, 89(D7), 11,749–11,757, doi:10.1029/JD089iD07p11749.
- Kerstel, E., and L. Gianfrani (2008), Advances in laser-based isotope ratio measurements: Selected applications, *Appl. Phys. B*, 92(3), 439–449, doi:10.1007/s00340-008-3128-x.
- Kerstel, E. R. T. (2004), Isotope ratio infrared spectrometry, in *Handbook of Stable Isotope Analytical Techniques*, edited by P. A. de Groot, chap. 34, pp. 759–787, Elsevier, Amsterdam.
- Kerstel, E. R. T., R. Q. Iannone, M. Chenevier, S. Kass, H.-J. Jost, and D. Romanini (2006), A water isotope (<sup>2</sup>H, <sup>17</sup>O, and <sup>18</sup>O) spectrometer based on optical-feedback cavity enhanced absorption for *in situ* airborne applications, *Appl. Phys. B*, 85(2–3), 397–406, doi:10.1007/s00340-006-2356-1.
- Lee, X., S. Sargent, R. Smith, and B. Tanner (2005) In situ measurement of the water vapor <sup>18</sup>O/<sup>16</sup>O isotope ratio for atmospheric and ecological applications, *J. Atmos. Oceanic Technol.*, 22, 555–565, doi:10.1175/JTECH1719.1.
- Majoube, M. (1971), Fractionnement en oxygène-18 et en deutérium entre l'eau et sa vapeur, *J. Chem. Phys.*, 197, 1423–1436.
- Meijer, H., and W. Li (1998), The use of electrolysis for accurate <sup>17</sup>O and <sup>18</sup>O isotope measurements in water isotopes, *Isotopes Environ. Health Stud.*, 34, 349–369, doi:10.1080/10256019808234072.
- Morville, J., S. Kass, M. Chenevier, and D. Romanini (2005), Fast, low-noise, mode-by-mode, cavity-enhanced absorption spectroscopy by diode-laser self-locking, *Appl. Phys. B*, 80, 1027–1038, doi:10.1007/s00340-005-1828-z.
- Rothman, L. S., et al. (2005), The HITRAN molecular spectroscopic database, *J. Quant. Spectrosc. Radiat. Transf.*, 96, 139–204, doi:10.1016/j.jqsrt.2004.10.008.
- Uemura, R., Y. Matsui, K. Yoshimura, H. Motoyama, and N. Yoshida (2008), Evidence of deuterium excess in water vapor as an indicator of ocean surface conditions, *J. Geophys. Res.*, 113, D19114, doi:10.1029/2008JD010209.
- Wang, L., K. K. Caylor, and D. Dragoni (2009), On the calibration of continuous, high-precision <sup>δ</sup><sup>18</sup>O and <sup>δ</sup><sup>2</sup>H measurements using an off-axis integrated cavity output spectrometer, *Rapid Commun. Mass Spectrom.*, 23, 530–536, doi:10.1002/rcm.3905.
- Wang, X. F., and D. Yakir (2000), Using stable isotopes of water in evapotranspiration studies, *Hydrol. Process.*, 14(8), 1407–1421, doi:10.1002/1099-1085(20000615)14:8<1407::AID-HYP992>3.0.CO;2-K.
- Wen, X.-F., X.-M. Sun, S.-C. Zhang, G.-R. Yu, S. D. Sargent, and X. Lee (2008), Continuous measurement of water vapor D/H and <sup>18</sup>O/<sup>16</sup>O isotope ratios in the atmosphere, *J. Hydrol. Amsterdam*, 349, 489–500, doi:10.1016/j.jhydrol.2007.11.021.
- White, J. W. C., and S. D. Gedzelman (1984), The isotopic composition of atmospheric water vapor and the concurrent meteorological conditions, *J. Geophys. Res.*, 89(D3), 4937–4939, doi:10.1029/JD089iD03p04937.
- Worden, J. R., et al. (2007), Importance of rain evaporation and continental convection in the tropical water cycle, *Nature*, 445, 528–532, doi:10.1038/nature05508.
- O. Cattani, LSCE, IPSL CEA Saclay, 91191 Gif sur Yvette, France.
- R. Q. Iannone, E. R. Th. Kerstel, and H. A. J. Meijer, Centrum voor IsotopenOnderzoek, University of Groningen, NL-9747 AG Groningen, Netherlands. (e.r.t.kerstel@rug.nl)
- D. Romanini, Laboratoire de Spectrométrie Physique, UMR 5588, Université J. Fourier Grenoble, CNRS, 38402 Saint Martin d'Hères, France.